Microfiber-probe-based ultrasmall interferometric sensor

Jun-long Kou, Jing Feng, Qian-jin Wang, Fei Xu,* and Yan-qing Lu

College of Engineering and Applied Sciences and National Laboratory of Solid State Microstructures, Nanjing University, Nanjing 210093, China

**Corresponding author: feixu@nju.edu.cn*

Received April 22, 2010; accepted June 1, 2010;
posted June 17, 2010 (Doc. ID 127408); published June 30, 2010

We report an ultrasmall microfiber-probe-based reflective interferometer for highly sensitive liquid refractive index measurement. It has a 3.5 μm micronotch cavity fabricated by focused ion beam micromachining. A sensitivity of 110 nm/RIU (refractive index unit) in liquid is achieved with over 20 dB extinction ratio. Theoretical analysis shows this kind of device is a hybrid of Fabry–Perot and modal interferometers. In comparison with normal fiber interferometers, this probe sensor is very compact, stable, and cheap, offering great potentials for detecting inside sub-wavelength bubbles, droplets, or biocells. © 2010 Optical Society of America

OCIS codes: 060.2370, 280.4788.

Optical fiber interferometers have been extensively used in various sensing applications due to their advantages of versatility, linear response, and relatively simple structure. In the past two decades, many efforts have been made to develop intrinsic and extrinsic interferometers, especially the microcavity Fabry–Perot interferometers (MCFPIs). MCFPIs with tens-of-micrometers-length cavities are attractive because of the small size, large free spectrum range (FSR), and high sensitivity. The cavity can be assembled by inserting a silica single-mode fiber (SMF) and a multimode fiber into a glass capillary [1], cascading Fabry–Perot cavities formed with a short piece of multimode fiber and a hollow core fiber [2], splicing two SMFs to a hollow-core fiber [3], or splicing an SMF and an index-guiding photonic crystal fiber together [4]. Although much progress has been made, people are still pursuing new microcavity fabrication techniques to improve the cavity length precision, structure accuracy, and the process repeatability. Femtosecond laser technology thus was proposed recently showing great success in micromachining fiber devices. MCFPIs can be quickly fabricated by drilling a small hole in an SMF for liquid and gas sensing [5]. However, even the femtosecond-laser-machined MCFPIs still show low fringe visibility of several decibels in liquids due to the rugged surfaces inside the cavity; what is more, it is difficult to focus the laser spot to a subwavelength scale owing to the diffraction limit [6]; thus the micromachining accuracy is limited and the size of the microcavity is large. The latest progress in focused ion beam (FIB) techniques has opened a new widow of opportunity for ultrasmall cavities. The fine and controllable ion spot size and high beam current density are perfect for nanofabrication. Microcavities with nanometer-scale accuracy in a subwavelength microfiber could be fabricated by FIB, which is relatively difficult for the femtosecond laser approach.

In this Letter, we demonstrated an ultrasmall inline reflective interferometric sensor with an open microcavity on the side of a single microfiber probe by direct FIB machining. The cavity has the dimensions of only several micrometers, which is much smaller than previous MCFPIs. A theoretical analysis reveals that this kind of device is a hybrid of Fabry–Perot and modal interferometers. Experimental results show our fiber probe interferometer has high extinction ratio and sensitivity. The compact size, simple fiber-probe structure, all fiber connection, and easy fabrication further make the microfiber-probe-based reflective interferometer (MPRI) a great candidate for chemical and biological sensing applications. It even could offer fantastic potential in detecting inside a biocell, thanks to its unique tiny probe structure.

Standard optical microfiber probes generally consist of tapered fiber tips and taper transitions. Since the microfiber probe is for analyte detecting rather than launching the light, it should be short enough in order to be rigid. However, too short and sharp a shape results in high losses owing to the poor adiabaticity of the taper profiles [7]. During the past decade, much work has been carried out to study and optimize microfiber taper profiles for telecom devices. Using a taper manufacturing rig it is possible to tailor the taper shape to an ideal profile [8], but it is not easy to fabricate a short fiber probe. In this work, we make taper probes using a commercial pipette puller (model P2000, Sutter Instrument). The fabrication process is simple, convenient [9], and extremely fast. The obtained microfiber taper probe is then checked under a microscope, as shown in Fig. 1. The profile is described by a decreasing local radius function $r(z)$, where z is the longitudinal coordinate. The origin of z is at the beginning of the taper transition. The length of the taper probe is about 2 mm, and the diameter r_0 at the end of the tip is less than 500 nm.

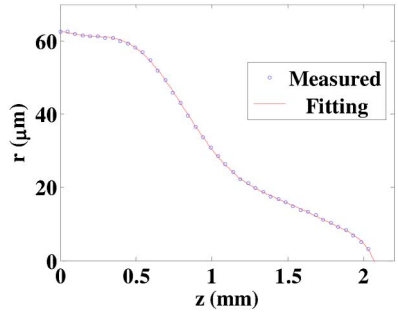

Fig. 1. (Color online) Taper profile measured (filled circles) under an optical microscope. The solid curve is a fitting curve.

The microfiber probe tip was coated with a thin aluminum (Al) layer and then was placed rigidly in the FIB machining chamber (Strata FIB 201, FEI company, 30 keV Ga ions) using conductive tape. We used a 30.0 kV, 288 pA gallium ion beam perpendicular to the fiber axis z to mill a micronotch cavity as illustrated in Fig. 2. This enabled us to make a micronotch with high accuracy and sharp end faces. Finally, the microfiber probe with a cavity was immersed in hydrochloric acid for about 25 min to totally remove the Al layer before cleaning with deionized water. An SEM image of the MPRI is shown in Fig. 2. The cavity is 3.50 μm long and 2.94 μm high, located at the position with the local radius $r = 2.4$ μm.

The experimental setup is shown in Fig. 3(a) to characterize the MPRI. A broadband source centered at 1550 nm is connected with an MPRI through an optical circulator. The light was reflected at the two end faces of the cavity [Fig. 3(b)], and the reflected spectra were measured by an optical spectrum analyzer (OSA). When the microfiber probe tip without a cavity before FIB machining was employed, almost no light was detected, showing a black background. However, an interference pattern was observed, as shown in Fig. 4(a), after the cavity was milled. The interference spectra of the MPRI in air, acetone, and isopropanol at 25 °C are recorded. The interference spectrum indicates a fringe visibility maximum of ~20 dB, which is much higher than those of typical MCFPIs in liquids.

Owing to the low reflectivity of the liquid–glass interfaces, multiple reflections have negligible contributions to the optical interference. As with previous standard fiber microcavity Fabry–Perot interferometers, this kind of device can be modeled using a two-beam optical interference equation $I = I_L + I_R + 2\sqrt{I_L I_R}\cos(\delta + \varphi_0)$, where I is the intensity of the interference signal; I_L and I_R are the reflections at both the two end faces L and R, respectively; φ_0 is the initial phase of the interference; $\delta = 4\pi n_c L_c/\lambda$ is the phase difference of the two backreflections; L_c is the length of the cavity; n_c is the index of the liquid in the cavity; and λ is the wavelength. The periodic fringe spacing or FSR $= \lambda^2/(2n_c L_c) \approx 243$ nm. In our calculation, $\lambda = 1530$ nm, $L_c = 3.5$ μm, and $n_c = 1.3739$.

In Fig. 4(b), the adjacent valley space is about 10 nm, and the intensities at the valleys decrease with increasing wavelength; this device is in fact a multi-beam optical interferometer. It is not only a simple Fabry–Perot interferometer but also a modal interferometer. Because the microfiber probe is possibly nonadiabatic [7,10], the fundamental mode LP_{01} can be coupled to the higher-order local cladding mode LP_{0m} with down-tapering at the taper transition, and the reflected LP_{0m} mode can be coupled back to the LP_{01} mode with up-tapering [7]; the reflected $LP_{01}(LP_{0m})$ mode from end face R also can be excited to the $LP_{01}(LP_{0m})$ mode and even other higher-order modes into end face L. Additionally, the visibility of the MPRI in liquid is higher than the one in air, because it is easier for mode exciting and coupling.

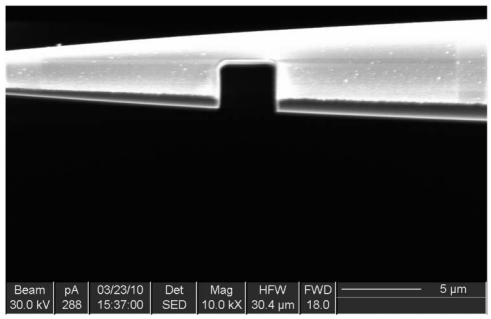

Fig. 2. SEM image of the micronotch cavity from the side.

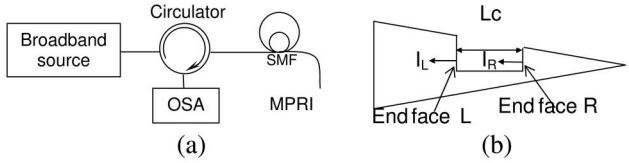

Fig. 3. (a) Experimental setup of an MPRI sensor. (b) Structure of an MPRI: I_L and I_R are the reflections at end face L and end face R, respectively, and L_c is the length of the cavity.

The phase differences between any two light beams are

$$\delta_{m,n} = p\delta_1 + q\delta_2 = 2pn_cL_c(2\pi/\lambda) + (2q\pi/\lambda)\int (n_2(r) - n_1(r))\mathrm{d}z(r),$$

where $p = 0$, 1 and $q = 0$, 1, 2; δ_1 and δ_2 are the phase difference because of the microcavity and the modal difference in the taper transition, respectively; $n_1(r)$ and $n_2(r)$ are the effective index of LP_{01} and LP_{0m} modes, respectively; and $n_1(r)$ and $n_2(r)$ are functions of local radius $r(z)$ of the microfiber probe at position z, which can be calculated by a three-layer model of finite cladding step-profile fiber with the microfiber probe profile $r(z)$ in Fig. 1 [7]. The estimated δ_1 is $\sim 13\pi$ and δ_2 $\sim 15\pi$ for the modal difference between the LP_{01} and LP_{02} modes.

The sensitivity S was measured by inserting the sensor in mixtures of isopropanol and acetone. These solutions were chosen with the objective of simulating aqueous solutions having a refractive index in the region around 1.33 at a wavelength of $\lambda = 1.55$ μm. The ratio was increased by adding small calibrated quantities of isopropyl to the solution at a position far from the sensor. The refractive indexes of pure isopropyl and acetone at 1.55 μm are 1.3739 and 1.3577, respectively [11].

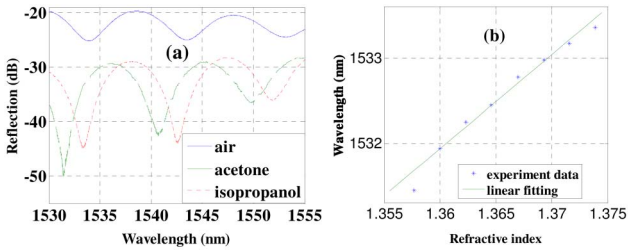

Fig. 4. (Color online) (a) Interference spectra of the MPRI device in air (solid curve), acetone (dashed curve), and isopropanol (dotted curve) at room temperature (25 °C). (b) The shifted spectral wavelength as a function of the liquid mixture refractive index. The asterisks represent the measured results while the solid curve is the fitting results.

Figure 4(b) displays the shifted spectral wavelength as a function of the liquid mixture refractive index. The asterisks represent the measurement results, while the solid curve is the best fit. As the refractive index increases, the spectrum shows a redshift. The sensitivity of the device is 110 nm/RIU (refractive index unit) according to Fig. 4(b). Higher sensitivity can be obtained by optimizing the profile of the microfiber taper probe.

We have demonstrated a microfiber-probe-based refractive interferometer sensor with an open micronotch cavity fabricated by FIB micromachining for highly sensitive refractive index measurement. Several experiments were carried out to study its sensing properties; the device has high extinction ratio (~20 dB) and sensitivity ~110 nm/RIU) in liquids. A theoretical analysis shows this kind of device is a hybrid of Fabry–Perot and modal interferometers. Owing to its small size, fiber-probe structure, all-fiber connection, linear response, low cost, easy fabrication, and high sensitivity, MPRI devices are promising in various chemical and biological applications. It even may offer fantastic potential for sensing inside subwavelength liquid droplets, bubbles, or biocells because of its unique probe structure and possible smaller size.

This work is sponsored by National 973 program under contract nos. 2010CB327800 and 2006CB921805, and the National Science Foundation of China (NSFC) program under contract nos. 60977039 and 10874080. The authors also acknowledge the support by Program for New Century Excellent Talents in University and Changjiang scholars program. We also thank Mr. Liang Ye for his technical support.

References

1. V. Bhatia, K. A. Murphy, R. O. Claus, M. E. Jones, J. L. Grace, T. A. Tran, and J. A. Greene, Measure. Sci. Technol. **7**, 58 (1996).
2. H. Y. Choi, G. Mudhana, K. S. Park, U.-C. Paek, and B. H. Lee, Opt. Express **18**, 141 (2010).
3. J. S. Sirkis, D. D. Brennan, M. A. Putman, T. A. Berkoff, A. D. Kersey, and E. J. Friebele, Opt. Lett. **18**, 1973 (1993).
4. J. Villatoro, V. Finazzi, G. Coviello, and V. Pruneri, Opt. Lett. **34**, 2441 (2009).
5. Y.-J. Rao, M. Deng, D.-W. Duan, X.-C. Yang, T. Zhu, and G.-H. Cheng, Opt. Express **15**, 14123 (2007).
6. K. M. Zhou, D. J. Webb, C. B. Mou, M. Farries, N. Hayes, and I. Bennion, IEEE Photon. Technol. Lett. **21**, 1653 (2009).
7. J. D. Love, W. M. Henry, W. J. Stewart, R. J. Black, S. Lacroix, and F. Gonthier, IEE Proc. J **138**, 343 (1991).
8. G. Brambilla, V. Finazzi, and D. J. Richardson, Opt. Express **12**, 2258 (2004).
9. G. Brambilla and F. Xu, Electron. Lett. **43**, 204 (2007).
10. Y. Jung, G. Brambilla, and D. J. Richardson, Opt. Express **16**, 14661 (2008).
11. T. Wei, Y. Han, Y. Li, H.-L. Tsai, and H. Xiao, Opt. Express **16**, 5764 (2008).